

Tissue Engineering

Tissue Engineering Manuscript Central: <http://mc.manuscriptcentral.com/ten>

A comparative study of shear stresses in collagen-GAG and calcium phosphate scaffolds in bone tissue-engineering bioreactors

Journal:	<i>Tissue Engineering</i>
Manuscript ID:	TEN-2008-0204.R1
Manuscript Type:	Original Article
Date Submitted by the Author:	n/a
Complete List of Authors:	Jungreuthmayer, Christian; Royal College of Surgeons in Ireland, Department of Anatomy; Trinity College Dublin, Department of Mechanical and Manufacturing Engineering; Siemens Medical Ireland Donahue, Seth; Michigan Technological University, Biomedical Engineering Jaasma, Michael; Royal College of Surgeons in Ireland, Department of Anatomy; Trinity College Dublin, Department of Mechanical and Manufacturing Engineering Al-Munajjed, Amir; Royal College of Surgeons in Ireland, Department of Anatomy; Trinity College Dublin, Department of Mechanical and Manufacturing Engineering Zanghellini, Jürgen; Karl Franzens University Graz, Institute of Chemistry Kelly, Daniel; Trinity College Dublin, Department of Mechanical Engineering OBrien, Fergal; Royal College of Surgeons in Ireland, Department of Anatomy; Trinity College Dublin, Department of Mechanical and Manufacturing Engineering
Keyword:	Tissue Development and Growth < Fundamentals of Tissue Engineering, Bone < Tissue Engineering Applications, Bioreactors < Enabling Technologies
Abstract:	The increasing demand for bone grafts combined with their limited availability and potential risks has led to much new research in bone tissue engineering. Current strategies of bone tissue engineering commonly utilize cell-seeded scaffolds and flow perfusion bioreactors to stimulate the cells to produce bone tissue suitable for implantation into the patient's body. The aim of this study was to quantify and compare the wall shear stresses in two bone tissue engineering scaffold types (collagen-GAG and calcium phosphate) exposed to fluid flow in a perfusion bioreactor. Based on μ CT images, 3D numerical CFD models of the two scaffold types were developed to calculate the wall shear stresses within the scaffolds. For a given flow rate (normalized by the cross-sectional area of the scaffolds), shear stress is 2.8-fold higher in the

collagen-GAG than the calcium-phosphate scaffold. This is due to the differences in scaffold geometry, particularly the pore size (collagen-GAG pore size $\sim 96\mu\text{m}$ and calcium phosphate pore size $\sim 350\mu\text{m}$). The numerically obtained results were compared to an analytical method which is widely used by experimentalists to determine perfusion flow rates in bioreactors. Our CFD simulations revealed that the cells in both scaffold types are exposed to a wide range of wall shear stresses throughout the scaffolds, and that the analytical method predicts shear stresses 12% to 21% greater than those predicted by the CFD method. The study has demonstrated that the wall shear stresses in calcium phosphate scaffolds (745.2mPa) are approximately 40 times higher than in collagen-GAG scaffolds (19.4mPa) when flow rates are applied which have been experimentally used to stimulate the release of PGE2. These findings indicate the importance of using accurate computational models to estimate shear stress and determine experimental conditions in perfusion bioreactors for tissue engineering.

Note: The following files were submitted by the author for peer review, but cannot be converted to PDF. You must view these files (e.g. movies) online.

jungreuthmayerTable4.eps



Review

1
2
3
4
5
6
7
8
9
10
11
12
13
14
15
16
17
18
19
20
21
22
23
24
25
26
27
28
29
30
31
32
33
34
35
36
37
38
39
40
41
42
43
44
45
46
47
48
49
50
51
52
53
54
55
56
57
58
59
60

A comparative study of shear stresses in collagen-GAG and calcium phosphate scaffolds in bone tissue-engineering bioreactors

Christian Jungreuthmayer^{1,2,3}, Seth W. Donahue⁴, Michael J. Jaasma^{1,2},
Amir A. Al-Munajjed^{1,2}, Jürgen Zanghellini⁵, Daniel J. Kelly²,
and Fergal J. O'Brien^{1,2}

¹ Department of Anatomy, Royal College of Surgeons in Ireland, Dublin 2,
Ireland

² Trinity Centre for Bioengineering, Department of Mechanical and
Manufacturing Engineering, Trinity College Dublin, Dublin 2, Ireland

³ Siemens Medical Ireland, Leeson Close, Dublin 2, Ireland

⁴ Department of Biomedical Engineering, Michigan Technological University,
Houghton, US

⁵ Institute of Chemistry, Karl Franzens University Graz, Graz, Austria

Address Correspondence and Reprints Requests to:

Professor Fergal J. O'Brien, PhD
Department of Anatomy
Royal College of Surgeons in Ireland
123 St. Stephen's Green
Dublin 2
Ireland
Phone: +353-(0)1-402-2149
Fax: +353-(0)1-402-2355
Email: fjobrien@rcsi.ie

Abstract

The increasing demand for bone grafts combined with their limited availability and potential risks has led to much new research in bone tissue engineering. Current strategies of bone tissue engineering commonly utilize cell-seeded scaffolds and flow perfusion bioreactors to stimulate the cells to produce bone tissue suitable for implantation into the patient's body. The aim of this study was to quantify and compare the wall shear stresses in two bone tissue engineering scaffold types (collagen-GAG and calcium phosphate) exposed to fluid flow in a perfusion bioreactor. Based on μ CT images, 3D numerical CFD models of the two scaffold types were developed to calculate the wall shear stresses within the scaffolds. For a given flow rate (normalized by the cross-sectional area of the scaffolds), shear stress is 2.8-fold higher in the collagen-GAG than the calcium-phosphate scaffold. This is due to the differences in scaffold geometry, particularly the pore size (collagen-GAG pore size $\sim 96\mu\text{m}$ and calcium phosphate pore size $\sim 350\mu\text{m}$). The numerically obtained results were compared to an analytical method which is widely used by experimentalists to determine perfusion flow rates in bioreactors. Our CFD simulations revealed that the cells in both scaffold types are exposed to a wide range of wall shear stresses throughout the scaffolds, and that the analytical method **predicts shear stresses 12% to 21% greater than those predicted by** the CFD method. The study has demonstrated that the wall shear stresses in calcium phosphate scaffolds (745.2mPa) are approximately 40 times higher than in collagen-GAG scaffolds (19.4mPa) when flow rates are applied which have been experimentally used to stimulate the release of PGE₂. These findings indicate the importance of using accurate computational

1
2
3 models to estimate shear stress and determine experimental conditions in
4
5
6 perfusion bioreactors for tissue engineering.
7
8
9
10
11
12
13
14
15
16
17
18
19
20
21
22
23
24
25
26
27
28
29
30
31
32
33
34
35
36
37
38
39
40
41
42
43
44
45
46
47
48
49
50
51
52
53
54
55
56
57
58
59
60

For Peer Review

Introduction

According to Laurencin *et al.* 500,000 bone replacement procedures were performed in the United States in 2005 of which 90% used either autografts or allografts ¹. Both autografts and allografts have substantial drawbacks.

Therefore, much recent focus of bone graft research is on bone tissue engineering, where cells (taken from the patient's bone marrow) are seeded onto a biological scaffold and growth factors are used to produce mineralized tissue *in vitro*. Alternatively, a bioreactor can be used to perfuse the cell-seeded scaffold with culture medium containing osteogenic growth factors. The fluid flow also provides biophysical stimulation which may enhance extracellular matrix deposition and mineralization of the construct to form bone tissue.

The scaffold biomaterial plays a key role in tissue engineering and the optimal scaffold has to combine a set of essential requirements such as biocompatibility, mechanical strength, and a highly porous microstructure and a pore size that allows cell migration and re-organization ². A wide variety of scaffold biomaterials has been studied over the past two decades including naturally occurring polymers (e.g. collagen, fibrin, and gelatin), synthetic polymers (e.g. polylactic acid (PLA) and polyglycolic acid (PGA)), and porous ceramics (e.g. bioglass® and calcium phosphate structures and naturally occurring ceramics, such as coral) ^{3,4}.

Previous work demonstrates that collagen-glycosaminoglycan (CG) ⁵ and calcium phosphate ⁶ scaffolds show promising results for bone tissue

1
2
3 engineering. Lyophilised CG scaffolds are characterized by very high porosity
4 (~99%), a high level of pore interconnectivity, excellent biodegradability and
5 biocompatibility. They can be produced with a wide range of homogeneous
6 pore sizes ^{7,8}. A disadvantage of the CG scaffold for bone tissue engineering
7 is that it has relatively poor mechanical properties. However, recent
8 investigations indicate that cross-linking methods can substantially improve
9 the mechanical stability of CG scaffolds ⁹. Among the positive features of
10 calcium phosphate scaffolds are their trabecular bone-like morphology and a
11 composition similar to bone mineral which results in excellent biocompatibility
12 ⁴. However, calcium phosphate scaffolds are brittle ^{4,10,11} and have a relatively
13 low porosity of 47% to 85% ¹² which limits cell penetration, nutrient delivery,
14 removal of metabolic waste products and subsequent vascularisation of new
15 tissue ⁴.

16
17
18
19
20
21
22
23
24
25
26
27
28
29
30
31
32
33
34
35
36
37 The mechanical stimulation caused by the fluid flow of the culture medium in a
38 bioreactor plays a critical role in anabolic bone cell activity. Wall stress acting
39 on osteoblastic cells activates bone formation activity *in vitro* ^{13,14}. The applied
40 wall shear stress needs to be in a physiologically relevant range. *In vivo*, bone
41 cells experience estimated shear stresses of 0.8Pa to 3.0Pa for the range of
42 routine physical activity ¹⁵. The effect of physiological shear stresses in 2D
43 cultures (i.e., parallel plate flow chambers) has been analysed in various
44 investigations ^{13,14,16,17}. These studies showed an increase of bone formation
45 markers, such as nitric oxide (NO) ¹⁴, prostaglandin E₂ (PGE₂) ^{13,14}, and
46 osteopontin (OPN) ^{16,17} due to the mechanical stimulation of osteoblasts
47 caused by the flow perfusion. In 2D experiments using parallel plate flow
48
49
50
51
52
53
54
55
56
57
58
59
60

1
2
3 chambers, all cells see approximately the same shear stress, which is easily
4
5
6 estimated by simple analytical methods because of the regular geometry of
7
8 the flow chamber. However, shear stress calculations are more complicated in
9
10 3D experiments because of complex scaffold geometries and an irregular flow
11
12 environment. In order to enable physiologically relevant shear stresses to be
13
14 accurately applied to cells in bioreactors, a computational approach can be
15
16
17 used to estimate the mechanical environment.
18

19
20
21
22 The calculation of the flow conditions within perfused highly irregular 3D
23
24 geometries is non-trivial. In general there are two approaches to determine
25
26 the shear stresses values: (i) analytical methods ^{18,19,20} and (ii) numerical
27
28 models ^{21,22}. Analytical methods are based on crude assumptions about the
29
30 scaffold geometry. Consequently, they offer only an estimation of the flow
31
32 conditions, are inherently inaccurate and do not provide a shear stress
33
34 distribution, whereas numerical approaches based on μ CT images of the
35
36 scaffolds can produce accurate solutions, but are time consuming and
37
38 computationally expensive.
39
40
41
42
43
44
45

46 Recently, two studies demonstrated the potential of using computational fluid
47
48 dynamics for investigating the flow conditions within 3D scaffolds for tissue
49
50 engineering. Cioffi et al. ²¹ used a μ CT based model to characterize the local
51
52 fluid dynamics to which chondrocytes are exposed in a perfusion bioreactor
53
54 for cartilage tissue engineering. They demonstrated that computational
55
56 modeling can be successfully used to quantify the shear stress which acts on
57
58 cells seeded on porous polyesterurethane scaffolds (with a pore diameter of
59
60

1
2
3 100 μ m and a porosity of 77%) in bioreactor experiments. Porter et al. ²²
4
5 utilized the Lattice-Boltzmann method ²³ to simulate the flow conditions within
6
7 perfused cell-seeded scaffolds. **They used** a μ CT scan of human trabecular
8
9 bone (pore diameter of 645 μ m) to define the **scaffold microstructure for the**
10
11 **simulation**. They demonstrated that scaffold pore size, porosity, and
12
13 dimensions and the **bioreactor architecture affect the wall shear stress**. **Their**
14
15 **results indicate that the experimental input flow rate alone cannot be used as**
16
17 **a basis for comparison of biological outcomes; in addition to the flow rate, the**
18
19 **contribution of scaffold architectural parameters must be considered**.
20
21
22
23
24
25
26

27 In this study we used 3D CFD models to investigate the fluid dynamics in CG
28
29 and calcium phosphate scaffolds, **which have been used in** flow perfusion
30
31 experiments ^{5,6}. These experiments demonstrated the potential of fluid shear
32
33 to stimulate bone cell activity in osteoblastic cell-seeded CG scaffolds ⁵ and
34
35 calcium phosphate scaffolds ⁶ in perfusion bioreactors. ~~Both of these studies~~
36
37 ~~were previously published in Tissue Engineering~~. In both studies, PGE₂
38
39 release by osteoblastic cells was stimulated by fluid flow shear. The boundary
40
41 conditions and parameters of the models presented here were chosen to
42
43 simulate the perfusion bioreactor experiments reported previously for CG ⁵
44
45 and calcium phosphate scaffolds ⁶. **It is important to note different flow rates**
46
47 **were used to stimulate the release of PGE₂ in those experiments**. A maximum
48
49 input flow rate of 1ml/min was used in the CG study ⁵, which resulted in the
50
51 stimulation of a PGE₂ value of ~3.5fg/DNA(pg), which was approximately a
52
53 20-fold increase over the **no-flow control group**. **In the calcium phosphate**
54
55 **scaffold study**, the much higher maximum input flow rate of 40ml/min caused
56
57
58
59
60

1
2
3 a PGE₂ level of ~2fg/DNA(pg), which was approximately a 5-fold increase
4
5 over the **no-flow** control group⁶. In the current study, CFD models of flow
6
7 through **the CG and calcium phosphate** 3D scaffolds were used to provide
8
9 accurate estimations of the shear stress that cells seeded on the scaffolds will
10
11 experience. ~~Accurate models are important for designing and interpreting~~
12
13 ~~results from experimental studies.~~ These models were used to address the
14
15 following questions: (i) What is the distribution of flow parameters (fluid
16
17 velocity and shear stress) in 3D scaffolds? (ii) How does the geometry (e.g.,
18
19 pore size and porosity) of two commonly used bone scaffolds (CG and
20
21 calcium phosphate) affect the distribution of flow parameters? (iii) How good is
22
23 the agreement between the results obtained using the analytical method
24
25 reported by Goldstein ¹⁸ and the CFD simulations?
26
27
28
29
30
31
32
33
34
35
36
37
38
39
40
41
42
43
44
45
46
47
48
49
50
51
52
53
54
55
56
57
58
59
60

Methods

Analytical and computational approaches were used to estimate the shear stresses that bone cells seeded on CG and calcium phosphate scaffolds are exposed to in perfusion bioreactors. The first method used the analytical approach according to Goldstein et al.¹⁸. The second method was a 3D computational fluid dynamics (CFD) model based on micro-computed tomography (μ CT) images of the two scaffolds.

The analytical method¹⁸ is based on the assumption that the scaffold can be represented as a bundle of parallel circular pipes. The diameter of each pipe, d_{pipe} , is equal to the average pore diameter, $d_{\text{pore}} = 2 \cdot r_{\text{pore}}$, of the scaffold. The average fluid velocity inside the scaffold, u_{scaf} , can be estimated by

$$u_{\text{scaf}} = Q / (\pi \cdot r_{\text{chamber}}^2 \cdot \Phi), \quad (1)$$

where Q is the inlet flow rate applied to the bioreactor, r_{chamber} is the radius of the bioreactor's scaffold chamber and Φ is the porosity of the scaffold. In the case of laminar fluid flow, the flow profile inside the pipes is parabolic: $u(r) = u_{\text{max}} \cdot (1 - r^2 / r_{\text{pipe}}^2)$ and the shear stress τ is given by

$$\tau = \mu \cdot du(r) / dr, \quad (2)$$

where μ is the dynamic viscosity of the culture medium. Calculating the gradient, $du(r) / dr$, at the pipe wall, $r = r_{\text{pipe}}$, and using the relation $u_{\text{max}} = 2 \cdot u_{\text{avg}} = 2 \cdot u_{\text{scaf}}$ we obtain for the wall shear stress τ

$$\tau = 8 * \mu * u_{\text{scaf}} / d_{\text{pore}}. \quad (3)$$

In the analytical calculations presented in this study, the scaffold's porosities were obtained from the μ CT scans and a dynamic viscosity of 0.001 Pa·s was used, which is in the range of commonly used culture media for flow perfusion bioreactor experiments in tissue engineering²⁴. In order to determine the analytical estimates for the CG scaffold a fluid velocity of 235 μ m/s and an average pore size of 96 μ m was used, which corresponds to the experimental settings of Jaasma and O'Brien⁵. The applied fluid velocity, u_{scaf} , was calculated by $u_{\text{scaf}} = Q/A_{\text{chamber}} = 1 \text{ ml/min} / (r_{\text{chamber}}^2 * \pi) = 1.667 \times 10^{-8} \text{ m}^3/\text{s} / [(0.00475 \text{ m})^2 * \pi] = 0.000235 \text{ m/s}$, where an input flow rate $Q=1 \text{ ml/min}$ and a chamber radius $r_{\text{chamber}}=4.75 \text{ mm}$ was used. The analytical results of the calcium phosphate scaffold were obtained by using an fluid velocity of 24.89 mm/s and an average pore size of 350 μ m corresponding to the experimental values of Vance et al.⁶. The applied fluid velocity u_{scaf} was calculated by $u_{\text{scaf}} = Q/A_{\text{chamber}} = 40 \text{ ml/min} / (r_{\text{chamber}}^2 * \pi) = 6.667 \times 10^{-7} \text{ m}^3/\text{s} / [(0.00292 \text{ m})^2 * \pi] = 0.02489 \text{ m/s}$, where an input flow rate $Q = 40 \text{ ml/min}$ and a scaffold chamber radius $r_{\text{chamber}} = 2.92 \text{ mm}$ was used. In order to improve the accuracy of the analytical estimation, the effective porosity $\Phi' = 1 - V_{\text{scaf_material}} / (h_{\text{scaf}} * A_{\text{chamber}})$ of the scaffold was used instead of the scaffold's real porosity $\Phi = 1 - V_{\text{scaf_material}} / V_{\text{scaf_entire}}$, where h_{scaf} is the height of the scaffold, A_{chamber} is the area of the bioreactor's scaffold chamber, $V_{\text{scaf_material}}$ is the total volume of the scaffold material, and $V_{\text{scaf_entire}}$ is the entire volume of the scaffold (volume of the scaffold material and of the scaffold's interstice).

1
2
3
4
5
6 Figure 1(a-d) show μ CT images of the CG and calcium phosphate scaffolds.
7
8 1(a) and (b) show 3D views and Figure 1 (c) and (d) cross sections of the
9
10 scaffolds. The images (resolution = $12\mu\text{m}$) of the radio-absorbent calcium
11
12 phosphate scaffolds were taken on a Scanco Medical 40 Micro CT system
13
14 with 70kVp X-ray source and $112\mu\text{A}$. The μ CT scans (resolution = $5\mu\text{m}$) of the
15
16 nearly radio-translucent CG scaffolds were performed by SCANCO Medical
17
18 AG in Bassersdorf/Switzerland using a special filter technology to increase the
19
20 contrast of the CG material. The key parameters of the scaffolds are listed in
21
22 Table 1. Both CFD models are based on μ CT images. The μ CT grey scale
23
24 raw data were filtered using a Gaussian rank filter and a threshold procedure
25
26 was performed to transform the grey scale representation of the scaffolds to
27
28 black-and-white geometries. Hexahedral meshes of the scaffold's interstices
29
30 were created after applying a marching-cube-like smoothing process to the
31
32 structure.
33
34
35
36
37
38
39
40

41 The huge demand on the mesh resolution (caused by the low inter-struts-
42
43 distance) and the high interstice volume of the CG scaffold prevented us from
44
45 being able to perform CFD simulations of the entire CG scaffold including the
46
47 bioreactor's scaffold chamber, the inlet pipe and the outlet pipe. Instead
48
49 simulations of three randomly chosen sub-volumes with a size of $640\mu\text{m} \times$
50
51 $640\mu\text{m} \times 480\mu\text{m}$ were performed (see Figure 2). In order to avoid boundary,
52
53 artifacts only results of an inner cube of $320\mu\text{m} \times 320\mu\text{m} \times 320\mu\text{m}$ have been
54
55 used for further investigations²¹. An inlet area of a length of $100\mu\text{m}$ was
56
57 added on top of the scaffold to allow the entering fluid flow to distribute freely.
58
59
60

1
2
3 The meshes of the CG scaffolds contained approximately 1.7 million
4
5 hexahedral elements with a mean side length of 4.7 μ m. A constant inlet
6
7 velocity of 235 μ m/s (corresponding to the maximum inlet flow rate of 1ml/min
8
9 used by Jaasma and O'Brien ⁵) was applied. A FEM deformation simulation of
10
11 the scaffold was performed which showed that the relative deformation of the
12
13 scaffold caused by the fluid flow is less than 0.2%, which leads to negligible
14
15 changes in the flow conditions within the scaffold. It has been established that
16
17 bone cells are more sensitive to fluid shear stress than substrate-strain
18
19 loading ^{25,26}, with *in vitro* substrate strains above 1.0% required to stimulate
20
21 bone cells to release signaling molecules ^{14,27}. In this study, the deformation
22
23 of the scaffold was neglected and the scaffold walls were assumed to be rigid
24
25 and impermeable.
26
27
28
29
30
31
32
33

34 Given the differences in porosity, it was possible to simulate the entire calcium
35
36 phosphate scaffolds including the scaffold chamber and part of the inlet and
37
38 outlet pipes (see Figure 3). Three simulations were performed using the μ CT
39
40 scans of three different calcium phosphate scaffolds. The meshes of each
41
42 CFD model contained approximately 8 million hexahedral elements with a
43
44 mean side length of 23.8 μ m. A constant inlet velocity of 53.8mm/s was
45
46 applied at the inlet pipe (corresponding to the maximum inlet flow rate of
47
48 40ml/min used by Vance et al. ⁶). Calcium phosphate is a rigid and brittle
49
50 material. Hence, in the CFD model the walls of calcium phosphate scaffold
51
52 were assumed to be rigid and impermeable.
53
54
55
56
57
58
59
60

1
2
3 The bioreactor designs of Jaasma and O'Brien⁵ and Vance et al.⁶ have many
4 similarities. Both concepts used a programmable syringe pump to perfuse
5 culture medium through the inlet pipe into the scaffold chamber where the
6 fluid perfused the cell-seeded scaffold. The culture medium exited the scaffold
7 chamber through an outlet pipe and was stored in a medium reservoir. The
8 main difference of the two designs concerned the scaffold chamber (see
9 Figure 4). Jaasma and O'Brien⁵ used an O-ring to ensure that the whole
10 culture medium flowed through and did not by-pass the CG scaffold. Vance et
11 al.⁶, however, used a different approach. They chose a diameter for the
12 scaffold chamber that resulted in a gap of approximately 350 μ m between the
13 chamber wall and the scaffold. The size of the gap was chosen to be equal to
14 the mean pore diameter in order to create similar flow conditions in the outer
15 region and the center of the calcium phosphate scaffold. The design
16 difference had two effects on our CFD models: (i) it was necessary to simulate
17 the entire calcium phosphate scaffold, including the scaffold chamber, in order
18 to determine whether the flow conditions in the outer region of the scaffold are
19 equal to the center of the scaffold, (ii) it was reasonable to simulate only sub-
20 volumes of the CG scaffolds, because the O-rings guaranteed that no culture
21 medium flowed around the scaffold. This minimizes boundary effects between
22 the scaffold and the chamber wall and creates uniform flow conditions over
23 the whole volume of the CG scaffold.
24
25
26
27
28
29
30
31
32
33
34
35
36
37
38
39
40
41
42
43
44
45
46
47
48
49
50
51
52
53
54

55 For both scaffold types the following standard CFD parameters and settings
56 were used: laminar flow, incompressible Newtonian fluid with a viscosity of
57 0.001Pa·s, no-slip scaffold and bioreactor walls, constant velocity inlet, and
58
59
60

1
2
3 zero pressure outlet. The CFD simulations were performed using the laminar
4 flow solver *icoFoam* of the open source CFD tool box *OpenFOAM*. A mesh
5 resolution study was undertaken to ensure a sufficient mesh density. Starting
6 from coarse CFD meshes, the number of mesh elements was gradually
7 increased and the maximum change in the fluid velocity and the wall shear
8 stress with each increase was determined. The mesh density was increased
9 until the maximum change in the fluid velocity was below 1.0%, and the
10 maximum change in the wall shear stress was below 1.5% of the previous
11 value.
12
13
14
15
16
17
18
19
20
21
22
23
24
25
26

27 The CG and the calcium phosphate scaffolds were simulated on a 64bit Linux
28 computer cluster using 8 CPUs in parallel. The simulation of one sub-volume
29 of the CG scaffold took approximately 13 days. However, approximately 3
30 days were required to perform the simulation of one calcium phosphate
31 scaffold.
32
33
34
35
36
37
38
39
40
41
42
43
44
45
46
47
48
49
50
51
52
53
54
55
56
57
58
59
60

Results

Table 2 shows the analytical results for the three sub-volumes of the CG scaffold using an average scaffold pore size of $96\mu\text{m}$, a dynamic viscosity of $0.001\text{Pa}\cdot\text{s}$, and an fluid velocity of $235\mu\text{m}/\text{s}$ - corresponding to the experimental settings of Jaasma and O'Brien⁵. The analytically estimated mean fluid velocity inside the CG scaffold was $0.260\text{mm}/\text{s}$ and resulted in an estimated wall shear stress of 21.7mPa .

Table 3 shows the analytical results for the three different calcium phosphate scaffolds using an average pore size of $350\mu\text{m}$, a dynamic viscosity of $0.001\text{Pa}\cdot\text{s}$, and a fluid velocity of $24.89\text{mm}/\text{s}$ - corresponding to the experimental settings of Vance et al.⁶. The mean average fluid velocity in the calcium phosphate scaffolds is approximately 160 times higher than in the CG scaffolds (on average $39.5\text{mm}/\text{s}$ compared to $0.260\text{mm}/\text{s}$). The higher fluid velocity for calcium phosphate scaffolds is caused by a combination of the much higher inlet flow rate (contributes a 106-fold increase) and the lower porosity of the calcium phosphate scaffold (contributes a 1.6-fold increase). The estimated wall shear stress experienced by cells in the calcium phosphate scaffolds is 903.4mPa , which is 41.6 times higher than cells experienced in the CG scaffold.

Figure 5 shows the distributions of the magnitude of the fluid velocity within the scaffolds using CFD simulations. The distributions do not include the inlet and outlet areas of the simulation volumes. Figure 5(a) depicts the distributions of the three simulated sub-volumes of the CG scaffold. The mean

1
2
3 and maximum fluid velocity (averaged over all three sub-volumes) was
4
5 0.296mm/s and 1.316mm/s, respectively. Figure 5(b) shows the distributions
6
7 of the three calcium phosphate scaffolds. On average, the mean fluid velocity
8
9 inside these scaffolds was 47.9mm/s and the maximum fluid velocity was
10
11 248.5mm/s. The fluid velocity distributions of both scaffold types feature a
12
13 plateau-like shape from very low velocities up to approximately the mean fluid
14
15 velocity and a rapid decay for velocities higher than the mean fluid velocity.
16
17
18

19
20
21
22 Figure 6 depicts the wall shear stress distributions of (a) CG and (b) calcium
23
24 phosphate scaffolds. The wall shear stress acting on CG scaffolds ranges
25
26 from 0 to 90mPa, exhibiting a mean wall shear stress value of 19.4mPa
27
28 (averaged over all three simulated sub-volumes). The calcium phosphate
29
30 scaffolds experienced much higher wall shear stresses (mean value of
31
32 745.2mPa and maximum value of 3107mPa) as shown in Figure 5b. Both
33
34 distributions clearly show that cells throughout the scaffolds are not subjected
35
36 to the same wall shear stress values, but experience a wide range of shear
37
38 stresses.
39
40
41
42
43
44
45

46 Table 4 compares the results from the analytical method and the CFD
47
48 simulations. As shown in Table 4 the analytical approach predicts lower mean
49
50 fluid velocities within the scaffolds, however, higher mean wall shear stress
51
52 values. Furthermore, it can be seen that agreement between analytical and
53
54 CFD approaches is better for CG than for the calcium phosphate scaffold.
55
56
57
58
59
60

Discussion

In this study we developed CFD models of two scaffold types (CG and calcium phosphate), which have been used previously for bone tissue engineering applications, in order to determine the wall shear stresses to which cells seeded on these scaffolds are exposed to during flow perfusion bioreactor experiments. The aim of the study was to investigate the effect of the geometry of the two scaffold types on the flow conditions and how the numerical results compare to results obtained by the simple analytical method reported by Goldstein¹⁸.

The CFD simulations and their comparison with the analytical method revealed three important findings: (i) cells seeded on scaffolds are exposed to a wide range of wall shear stresses, (ii) the simple analytical method (compared to the CFD models) predicts higher wall shear stresses, and (iii) the fluid velocities and the wall shear stresses within scaffolds can vary greatly between different types of scaffolds because of differences in scaffold micro-structural geometries. All three findings are of importance for planning and performing bioreactor experiments for tissue engineering.

The highly irregular geometry of the scaffolds resulted in a complex fluid dynamics environment that causes a wide range of shear stress values (Figure 6). Although the analytical method suggests that all cells are exposed to the same shear stress value (by providing the mean shear stress value only), the CFD models show cells are exposed to a wide distribution of wall shear stresses. Hence, cells at different locations within the scaffold will be

1
2
3 exposed to different magnitudes of fluid shear. The whole range of shear
4
5 stress values was evenly distributed over the entire CG scaffold. High shear
6
7 stresses occurred on locations where the culture medium had to pass through
8
9 narrow channels and orifices, which resulted in an increased flow velocity and
10
11 thereby an increased wall shear stress. In the calcium phosphate scaffold the
12
13 highest wall shear stress values occurred at a ring-like region where the
14
15 scaffold touched the bottom of the bioreactor chamber creating a narrow flow
16
17 path which increased the wall shear stress.
18
19
20
21
22
23

24 The analytical method reported by Goldstein¹⁸ which is widely used by
25
26 experimentalists^{5,6} to calculate the wall shear stresses and to determine the
27
28 bioreactor's input flow rates, predicts shear stresses approximately 12% to
29
30 21% higher than the CFD simulations for the scaffolds investigated here. If
31
32 this method is used to design experiments, this difference might result in
33
34 bioreactor studies where the input flow rates are too low, leading to a lack of
35
36 osteogenic stimulation or a stimulation of osteogenic activity that is sub-
37
38 optimal. Better agreement to the numerical results might be found by using
39
40 the analytical method reported by Wang et al.²⁰. However, Wang's approach
41
42 requires the non-trivial measurement of the scaffold's Darcy permeability,
43
44 which introduces a new source of inaccuracy.
45
46
47
48
49
50

51
52 Both methods (CFD model and analytical estimation) revealed that the fluid
53
54 velocity and the wall shear stress largely differed between the two types of
55
56 scaffold. In order to compare the results with respect to the applied fluid flow,
57
58 the commonly reported input flow rate, Q , is inadequate due to its dependency
59
60

1
2
3 on the cross-sectional area of the scaffolds. Instead, we propose a normalized
4
5 input flow rate $q_{\text{norm}} = Q/A_{\text{scaf}}$ is used, which eliminates the influence of the
6
7 scaffold size. The mean velocity within the calcium phosphate scaffold was
8
9 approximately 160 times higher than in the CG scaffold (CG: $u_{\text{avg}} \approx$
10
11 0.296mm/s, calcium phosphate: $u_{\text{avg}} \approx 47.9\text{mm/s}$) mainly caused by the
12
13 **approximately 100-fold** higher input flow rate (CG: $q_{\text{norm}} = 0.235\text{mm/s}$, calcium
14
15 phosphate: $q_{\text{norm}} = 24.9\text{mm/s}$) and the **higher** porosity of the CG scaffold. The
16
17 mean wall shear stress was approximately 38 times higher **in calcium**
18
19 **phosphate scaffolds than in CG scaffolds** (CG: $\sim 20\text{mPa}$, calcium phosphate:
20
21 $\sim 750\text{mPa}$). The lower **percentage difference (between CG and calcium**
22
23 **phosphate scaffolds) in wall shear stress than in fluid velocity is likely due to**
24
25 **the** larger pore size and the less complex geometry of the calcium phosphate
26
27 scaffolds.
28
29
30
31
32
33

34
35
36 In order to obtain the same mean wall shear stress within both scaffold types
37
38 a 2.8-fold higher input flow rate (normalized by the cross-sectional area of the
39
40 scaffolds) is required in the calcium phosphate scaffold than the CG scaffold.
41
42 Despite the lower porosity of the calcium phosphate scaffold, a larger input
43
44 flow rate is required because of the less complex pore structure and the larger
45
46 pore size of the calcium phosphate scaffold. However, the input flow rates and
47
48 estimated mean wall shear stresses may not be sufficient for explaining biological
49
50 outcomes in different scaffold/bioreactor systems. For example, lower shear stresses
51
52 produced greater PGE_2 releases from osteoblasts in CG scaffolds ⁵ than from
53
54 osteoblasts exposed to higher shear stresses in calcium phosphate scaffolds ⁶. ~~In~~
55
56 ~~this study we used, for both scaffold types, input flow rates which were~~
57
58 ~~sufficient in recent experiments to detect increases in PGE_2 released by~~
59
60

1
2
3 ~~osteoblastic cells~~^{5,6}. The differences in wall shear stresses used to stimulate
4
5
6 PGE₂ release in the different scaffolds may be explained by the manner by
7
8 which cells attach to the scaffold²⁸. In scaffolds with large pores (e.g. calcium
9
10 phosphate scaffolds with a pore size of ~350μm) the cells are flatly attached
11
12 to scaffold wall⁶, whereas cells seeded on scaffolds with smaller pores (e.g.
13
14 CG with a pore size of ~96μm) can also bridge between two struts of the
15
16 scaffold^{29,30}. Bridging cells are more easily deformed than flatly attached cells
17
18 and therefore experience greater mechanical stimulation²⁸. **Therefore, the**
19
20 **greater PGE₂ release in the experiment with CG scaffolds may be due in part**
21
22 **to greater cell deformation.**
23
24
25
26
27
28

29
30 In the analytical method, the wall shear stress is determined by assuming that
31
32 the scaffold is made out of a bundle of parallel circular pipes. These pipes are
33
34 perfused by the culture medium with a mean fluid velocity u_{scaf} , which is
35
36 estimated by Equation 1. In bioreactor designs where the culture medium can
37
38 also flow around the scaffold (as in Figure 4(b)) the accuracy of estimation of
39
40 the wall shear stress using the analytical method can be significantly improved
41
42 if the radius of scaffold chamber is used, as in Equation 1, instead of using the
43
44 scaffold's radius⁶. Using the radius of the scaffold erroneously implies that the
45
46 fluid has to flow through a smaller cross-section and thereby causes a higher
47
48 mean fluid velocity and a higher wall shear stress. By using the chamber
49
50 radius instead of the scaffold radius, the difference in the estimated wall shear
51
52 stress relative to the wall shear stress obtained by the CFD simulation was
53
54 reduced from 48.3% ($\tau_{\text{analyt}}=1105.1\text{mPa}$) to 22.2% ($\tau_{\text{analyt}}=903.4\text{mPa}$).
55
56
57
58
59
60

1
2
3 The following limitations should be considered in the interpretation of this
4 work. (i) The CFD models did not account for molecular transport which can
5 affect mechanotransduction responses ³¹. (ii) The results of the CFD models
6 of the calcium phosphate scaffolds are likely more accurate than that of the
7 CG scaffold for two reasons: Firstly, the CFD model of the calcium phosphate
8 scaffolds contained the whole flow path including the bioreactor's scaffold
9 chamber and part of the inlet and outlet pipe, whereas the model of the CG
10 scaffolds only included a sub-volume of the entire scaffold and did not include
11 the bioreactor geometry. However, the effect on the results is considered to
12 be negligible as the bioreactor utilized O-rings to prevent fluid from flowing
13 around the scaffold ³² (see Figure 4). Secondly, the quality of the μ CT images
14 of the radio-absorbent calcium phosphate scaffolds was substantially better
15 than of the nearly radio-translucent CG scaffolds. The minimum pixel size of
16 $5\mu\text{m}$ of the used μ CT (which is in the range of the dimensions of the micro-
17 structures of the CG scaffold), combined with the poor radio-opaque
18 properties of CG resulted in a CFD model with a scaffold porosity of
19 approximately 90.5% compared to a porosity of 99% obtained by physical
20 measurement. (iii) The CFD simulations provide more insight about the
21 physical conditions within the scaffolds than the analytical approach because
22 the CFD simulations provide the distributions of velocities and shear stresses,
23 whereas the analytical approach only provides mean values. However, the
24 absolute and relative accuracy of both methods can only be evaluated by
25 comparing the theoretical results with data obtained by accurate experimental
26 measurements. The measurement of local flow conditions within highly
27 irregular micro-structures is non-trivial and was not performed in this study.
28
29
30
31
32
33
34
35
36
37
38
39
40
41
42
43
44
45
46
47
48
49
50
51
52
53
54
55
56
57
58
59
60

1
2
3
4
5
6 In conclusion this study shows that the flow conditions within two scaffolds
7
8 which have been used for bone tissue engineering applications are highly
9
10 irregular due to the complex scaffold geometries. These irregular flow
11
12 conditions lead to a wide range of wall shear stresses experienced by cells
13
14 seeded on these scaffolds. In order to subject the majority of the cells to
15
16 physiologically relevant wall shear stresses, the experimental setup (in
17
18 particular the determination of the input flow rate) must be chosen carefully.
19
20 The widely used analytical method reported by Goldstein et al. ¹⁸ predicts
21
22 higher wall shear stresses than the CFD approach and only yields a mean
23
24 value. Therefore, this analytical method is of limited use for setting up
25
26 bioreactor experiments. Our study also showed that the wall shear stress
27
28 used to stimulate PGE₂ release from osteoblastic cells in calcium phosphate
29
30 scaffolds is much higher than in CG scaffolds. This might be due to the
31
32 smaller pore size of the CG scaffolds which allows cells to not only attach
33
34 flatly on the scaffold wall but also to bridge between two struts of the scaffold,
35
36 which likely causes greater cell deformation than in cells seeded in scaffolds
37
38 with larger pore sizes such as the calcium phosphate scaffolds studied here
39
40 ²⁸. Our findings suggest that computational models can be of great value for
41
42 planning 3D bioreactor experiential conditions and interpreting results on
43
44 mechanically induced changes in bone cell metabolism. However, because of
45
46 the variability in scaffold and bioreactor geometries, custom CFD models need
47
48 to be developed for specific experimental configurations.
49
50
51
52
53
54
55
56
57
58
59
60

Acknowledgments

We would like to thank Dr. Alex Lennon for his technical support and assistance with the Linux computer cluster.

This project was funded by a Science Foundation Ireland Industry Research Partnership with Siemens.

For Peer Review

References

- [1] Laurencin, C., Khan, Y., and El-Amin, S. F. Bone graft substitutes. *Expert Review of Medical Devices* 3, 49, 2006
- [2] Stevens, B., Yang, Y., Mohandas, A., Stucker, B., and Nguyen, K. T. A review of materials, fabrication methods, and strategies used to enhance bone regeneration in engineered bone tissue. *Journal of Biomedical Materials Research Part B: Applied Biomaterials*, 17937408, 2007
- [3] Hutmacher, D. W., Schantz, J. T., Lam, C. X. F., Tan, K. C., and Lim, T. C. State of the art and future directions of scaffold-based bone engineering from a biomaterials perspective. *Journal of Tissue Engineering and Regenerative Medicine* 1, 245, 2007
- [4] Rezwan, K., Chen, Q. Z., Blaker, J. J., and Boccaccini, A. R. Biodegradable and bioactive porous polymer/inorganic composite scaffolds for bone tissue engineering. *Biomaterials* 27, 3413, 2006
- [5] Jaasma, M. J., and O'Brien, F. J. Mechanical stimulation of osteoblasts by steady and dynamic fluid flow. *Tissue Engineering*, accepted, 2008
- [6] Vance, J., Galley, D., Liu, D. F., and Donahue, S. W. Mechanical Stimulation of MC3T3 Osteoblastic Cells in a Bone Tissue-Engineering Bioreactor Enhances Prostaglandin E₂ Release. *Tissue Engineering* 11,1832, 2005
- [7] O'Brien, F. J., Harley, B. A., Yannas, I. V., and Gibson, L. Influence of freezing rate on pore structure in freeze-dried collagen-GAG scaffolds. *Biomaterials* 25,1077, 2004

- 1
2
3 [8] O'Brien, F. J., Harley, B. A., Yannas, I. V., and Gibson, L. The effect of
4 pore size on cell adhesion in collagen-GAG scaffolds. *Biomaterials* 26(4), 433,
5
6 2005
7
8
9
10 [9] Haugh, M. G., Jaasma, M. J., and O'Brien, F. J. The Effect of
11 Dehydrothermal Treatment on the Mechanical and Structural Properties of
12 Collagen-GAG scaffolds. *Journal of Biomedical Materials Research Part A*,
13
14 accepted, 2008
15
16
17
18
19 [10] Karageorgiou, V., and Kaplan, D. Porosity of 3D biomaterial scaffolds
20 and osteogenesis. *Biomaterials* 26, 5474, 2005
21
22
23
24 [11] Russias, J., Saiz, E., Deville, S., Gryn, K., Liu, G., Nalla, R. K., and
25 Tomsia, A. P. Fabrication and in vitro characterization of three-dimensional
26 organic/inorganic scaffolds by robocasting. *Journal of Biomedical Materials*
27
28
29
30
31
32
33 Research Part A 83(2), 434, 2007
34
35 [12] Baksh, D. A comparison of 3-dimensional calcium phosphate scaffolds
36 for candidate bone tissue engineering constructs [Master Thesis]. University
37 of Toronto, Toronto, Canada, 1999
38
39
40
41 [13] Bakker, A. D., Joldersma, M., Klein-Nulend, J., and Burger, E. H.
42 Interactive effects of PTH and mechanical stress on nitric oxide and PGE₂
43 production by primary mouse osteoblastic cells. *Am. J. Physiol. Endocrinol.*
44
45
46
47
48
49
50
51
52 [14] Smalt, R., Mitchell, F. T., Howard, R. L., and Chambers, T. J. Induction
53 of NO and prostaglandin E₂ in osteoblasts by wall-shear stress but not
54
55
56
57
58
59
60
mechanical strain. *Am. J. Physiol.* 273, E751, 1997

- 1
2
3 [15] Weinbaum, S., Cowin, S. C., and Zeng, Y. A model for the excitation of
4 osteocytes by mechanical loading-induced bone fluid shear stresses. J.
5 Biomech. 27, 339, 1994
6
7
8
9
10 [16] You, J., Reilly, G. C., Zhen, X., Yellowley, C. E., Chen, Q., Donahue, H.
11 J., and Jacobs, C. R. Osteopontin Gene Regulation by Oscillatory Fluid Flow
12 via Intracellular Calcium Mobilization and Activation of Mitogen-activated
13 Protein Kinase in MC3T3-E1 Osteoblasts. J. Biol. Chem. 276 (16), 13365,
14 2001
15
16
17
18
19
20
21
22 [17] Owan, I., Burr, D. B., Turner, C. H., Qiu, J., Tu, Y., Onyia, J. E., and
23 Duncan, R. L. Mechanotransduction in bone: osteoblasts are more responsive
24 to fluid forces than mechanical strain. Am J Physiol. 273, C810, 1997
25
26
27
28
29 [18] Goldstein, A. S., Juarez, T. M., Helmke, C. D., Custin, M. C., and
30 Mikos, A. G. Effect of convection on osteoblastic cell growth and function in
31 biodegradable polymer foam scaffolds. Biomaterials 22, 1279, 2001
32
33
34
35
36 [19] Botchwey, E. A., Pollack, S. R., El-Amin, S., Levine, E. M., Tuan, R. S.,
37 and Laurencin, C. T. Human osteoblast-like cells in three-dimensional culture
38 with fluid flow. Biorheology 40, 299, 2003
39
40
41
42
43 [20] Wang, S., and Tarbell, J. M. Effect of Fluid Flow on Smooth Muscle
44 Cells in a 3-Dimensional Collagen Gel Model. Arterioscler. Thromb. Vasc.
45 Biol. 20, 2220, 2000
46
47
48
49
50 [21] Cioffi, M., Boschetti, F., Raimondi, M. T., and Dubini, G. Modeling
51 Evaluation of the Fluid-Dynamic Microenvironment in Tissue-Engineered
52 Constructs: A Micro-CT Based Model. Biotechnology and Bioengineering
53 93(3), 500, 2005
54
55
56
57
58
59
60

- 1
2
3 [22] Porter, B., Zauel, R., Stockman, H., Guldborg, R., and Fyhrie, D. 3-D
4 computational modeling of media flow through scaffolds in a perfusion
5 bioreactor. J Biomech 38(3), 543, 2005
6
7
8
9
10 [23] Martys, N., and Chen, H. Simulation of multicomponent fluids in
11 complex three-dimensional geometries by the Lattice Boltzmann method.
12 Physics Review E53, 743, 1996
13
14
15
16
17 [24] Donahue, T. L., Haut, T. R., Yellowley, C. E., Donahue, H. J., and
18 Jacobs, C. R. Mechanosensitivity of bone cells to oscillating fluid flow induced
19 shear stress may be modulated by chemotransport. J Biomech 36, 1363,
20 2003
21
22
23
24
25
26
27 [25] Wang, Y., McNamara, L. M., Schaffler, M. B., and Weinbaum, S. A
28 model for the role of integrins in flow induced mechanotransduction in
29 osteocytes. PNAS 104(40), 15941, 2007
30
31
32
33
34 [26] McGarry, J. G., Klein-Nulend, J., Mullender, M. G., and Prendergast, P.
35 J. A comparison of strain and fluid shear stress in stimulating bone cell
36 responses – a computational and experimental study. FASEB Journal 19(3),
37 482, 2005
38
39
40
41
42
43 [27] You, J., Yellowley, C. E., Donahue, H. J., Zhang, Y., Chen, Q., and
44 Jacobs, C. R. Substrate Deformation Levels Associated With Routine Physical
45 Activity Are Less Stimulatory to Bone Cells Relative to Loading-Induced
46 Oscillatory Fluid Flow. J Biomechanical Engineering 122, 387, 2000
47
48
49
50
51
52
53 [28] Jungreuthmayer, C., Jaasma, M. J., Al-Munajjed, A. A., Zanghellini, J.,
54 Kelly, D. J., and O'Brien, F. J. 3D CFD-deformation simulation of a cell-
55 seeded collagen-GAG scaffold in a flow perfusion bioreactor. Medical
56 Engineering and Physics, submitted, 2008
57
58
59
60

1
2
3 [29] McMahon, L. The effect of cyclic tensile loading and growth factors on
4 the chondrogenic differentiation of bone-marrow derived mesenchymal stem
5 cells in a collagen-glycosaminoglycan scaffold [PhD thesis]. Trinity College
6 Dublin, Dublin, Ireland, 2007
7
8
9
10
11

12 [30] Freyman, T. M., Yannas, I. V., Pek, Y-S., Yokoo, R., and Gibson, L. J.
13 Micromechanics of Fibroblast Contraction of a Collagen-GAG Matrix.
14 Experimental Cell Research 269, 140, 2001
15
16
17
18

19 [31] Burger, J. H., and Klein-Nulend, J. Responses of bone cells to
20 biomechanical forces in vitro. Adv Dent Res 13, 93, 1999
21
22
23

24 [32] Jaasma, M. J., Plunkett, N. A., and O'Brien, F. J. Design and validation
25 of a dynamic flow perfusion bioreactor for use with compliant tissue
26 engineering scaffolds. J Biotechnology 133, 490, 2008
27
28
29
30
31
32
33
34
35
36
37
38
39
40
41
42
43
44
45
46
47
48
49
50
51
52
53
54
55
56
57
58
59
60

Table 1

Key parameters of the investigated CG and calcium phosphate scaffolds.

Table 2

The analytical results of the fluid velocity (u_{analyt}) and the wall shear stress (τ_{analyt}) for the CG scaffold using an fluid velocity of 235 $\mu\text{m/s}$, an average pore size of 96 μm , and a dynamic viscosity of 0.001Pa·s corresponding to the experimental settings of Jaasma and O'Brien ⁵.

Table 3

The analytical results of the calcium phosphate scaffold for the fluid velocity (u_{analyt}) and the wall shear stress (τ_{analyt}) using an fluid velocity of 24.89mm/s, an average pore size of 350 μm , and a dynamic viscosity of 0.001Pa·s corresponding to the experimental settings of Vance et al. ⁶.

Table 4

A comparison of the results from the analytical method and the CFD simulations. The displayed results are values averaged over the 3 samples of each scaffold type. E_{rel} indicates the error of the analytical approach relative to the CFD model.

Figure 1

3D views of the CG (a) and calcium phosphate scaffold (b). (c) and (d) show cross-sections of the CG and the calcium phosphate scaffold, respectively.

Figure 2

Three randomly chosen sub-volumes (640 μ m x 640 μ m x 480 μ m) were used to determine the flow conditions of the CG scaffold.

Figure 3

Three entire scaffolds including the scaffold chamber plus part of the inlet and outlet pipes were used to simulate the flow conditions of calcium phosphate scaffolds.

Figure 4

Sketches of the bioreactor's scaffold chambers according to Jaasma et al.^{5,31} using CG scaffolds (a) and Vance et al.⁶ using calcium phosphate scaffolds (b).

Figure 5

The distribution of the fluid velocity within (a) the CG and (b) the calcium phosphate scaffolds obtained from the CFD simulation. The distributions do not include the inlet and outlet areas of the simulation volume. The input flow rate of (a) was 1ml/min and of (b) was 40ml/min corresponding to recent experiments^{5,6}.

Figure 6

The distribution of the wall shear stress of the (a) CG and (b) the calcium phosphate scaffolds calculated using CFD models. In order to avoid boundary artefacts for the CG scaffolds only the data of inner cubes of $320\mu\text{m} \times 320\mu\text{m} \times 320\mu\text{m}$ have been used for the calculation of the shear stress distribution.

The input flow rate of (a) was 1ml/min and of (b) was 40ml/min corresponding to recent experiments^{5,6}.

For Peer Review

	CG	Calcium phosphate
avg. pore size [μm]	96	350
avg. porosity [%] (measured)	99	60
avg. porosity [%] (CFD)	90.5	58.5
scaffold diameter [mm]	9.5	5.0
scaffold height [mm]	3.5	3.9
scaffold volume [mm^3]	248.10	76.58
scaffold's interstice volume [mm^3] (measured)	245.61	49.78
scaffold's interstice volume [mm^3] (CFD)	223.78	44.80
bioreactor's chamber diameter [mm]	9.5	5.83

	Φ [%]	u_{analyt} [mm/s]	τ_{analyt} [mPa]
Sub-volume 1	92.4	0.254	21.2
Sub-volume 2	89.6	0.262	21.9
Sub-volume 3	89.4	0.263	21.9

For Peer Review

	Φ' [%]	u_{analyt} [mm/s]	τ_{analyt} [mPa]
Scaffold 1	67.11	37.09	847.8
Scaffold 2	60.45	41.17	941.0
Scaffold 3	61.74	40.31	921.4

For Peer Review

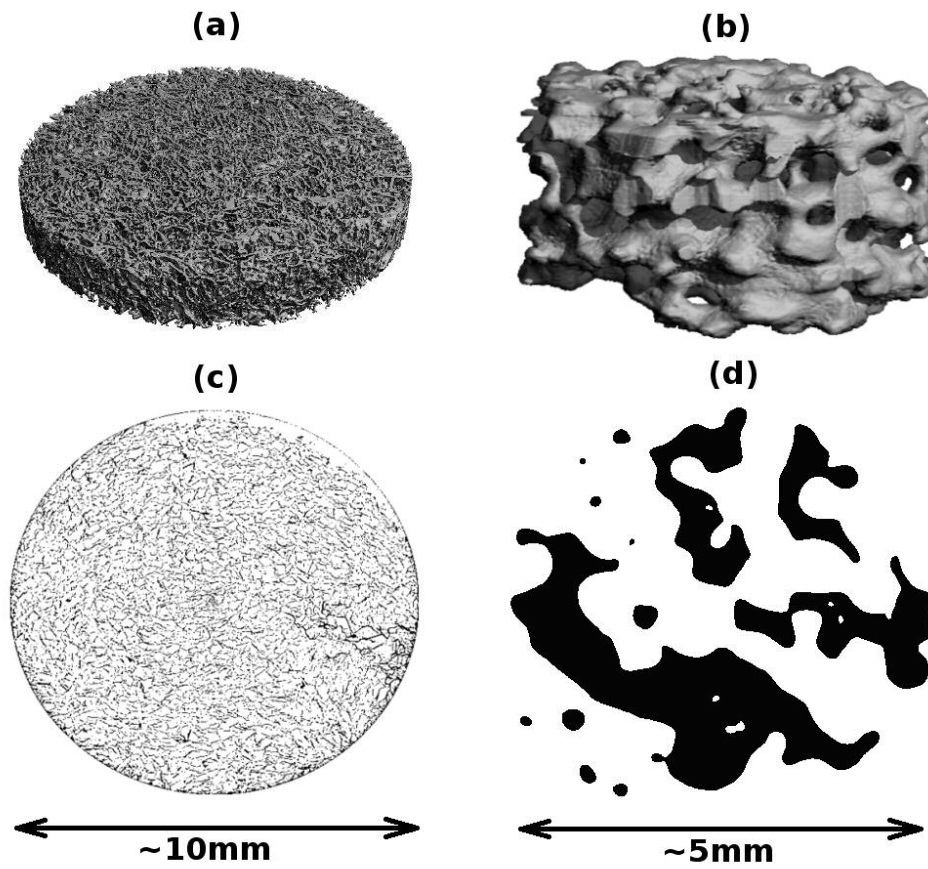


Figure 1
361x321mm (72 x 72 DPI)

1
2
3
4
5
6
7
8
9
10
11
12
13
14
15
16
17
18
19
20
21
22
23
24
25
26
27
28
29
30
31
32
33
34
35
36
37
38
39
40
41
42
43
44
45
46
47
48
49
50
51
52
53
54
55
56
57
58
59
60

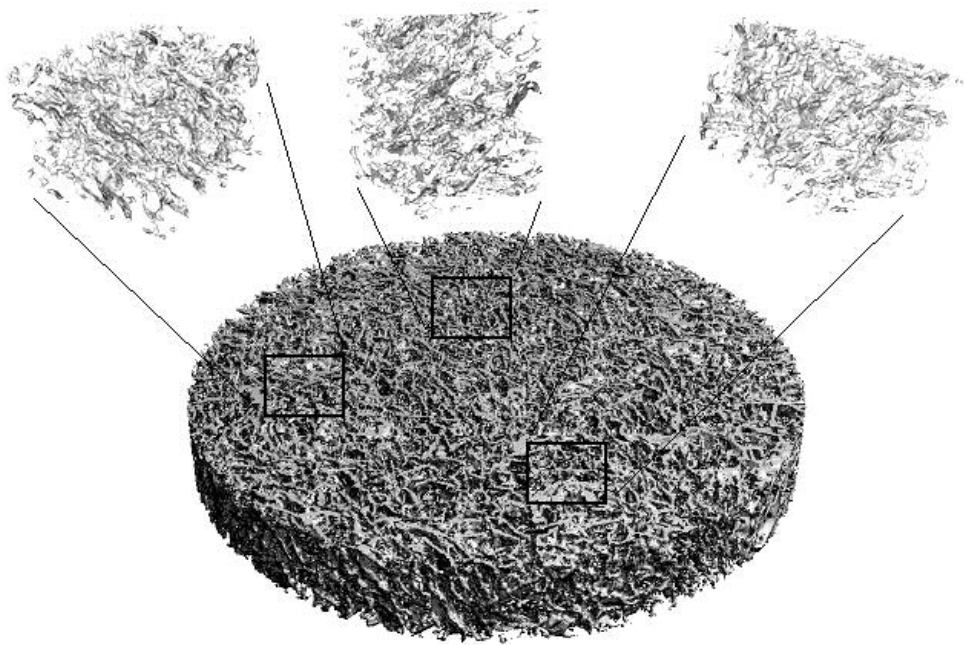


Figure 2

Review

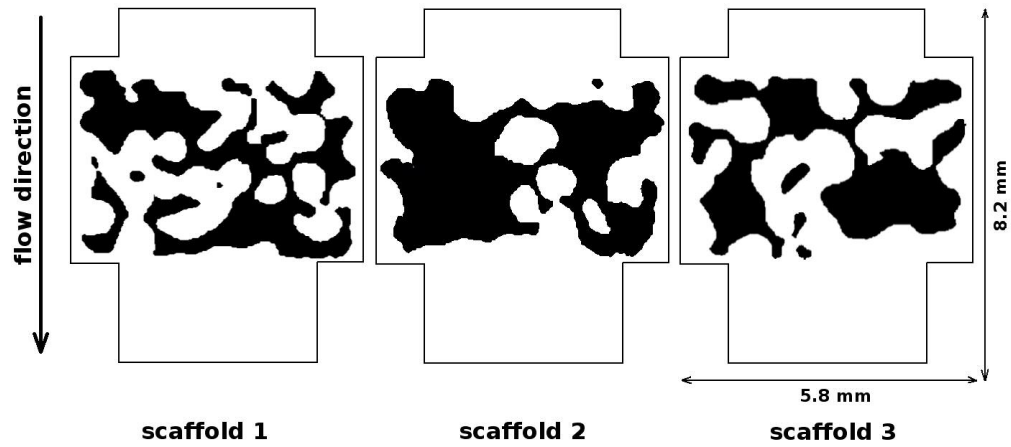


Figure 3

1
2
3
4
5
6
7
8
9
10
11
12
13
14
15
16
17
18
19
20
21
22
23
24
25
26
27
28
29
30
31
32
33
34
35
36
37
38
39
40
41
42
43
44
45
46
47
48
49
50
51
52
53
54
55
56
57
58
59
60

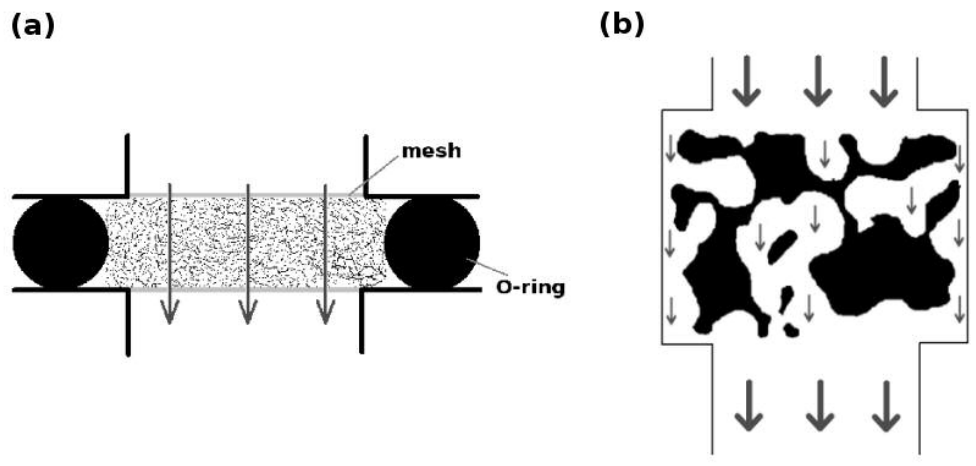
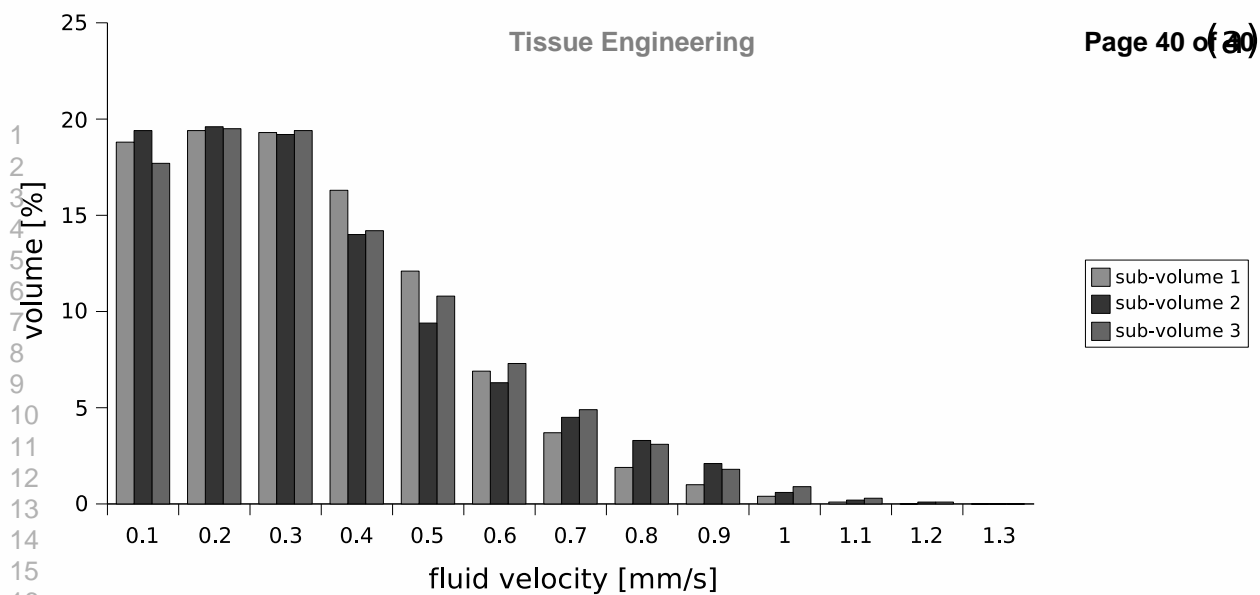


Figure 4

Peer Review

Tissue Engineering



(b)

